HHS Public Access

Author manuscript

Lab Chip. Author manuscript; available in PMC 2022 June 27.

Published in final edited form as:

Lab Chip. ; 22(7): 1310–1320. doi:10.1039/d2lc00030j.

A 3D-Printed Transfusion Platform Reveals Beneficial Effects of Normoglycemic Erythrocyte Storage Solutions and a Novel Rejuvenating Solution

Yueli Liu[1],

Laura E. Hesse[1],

Morgan K. Geiger[2,3],

Kurt R. Zinn[2,3],

Timothy J. McMahon[4],

Chengpeng Chen[5],

Dana M. Spence[2,3]

[1]Department of Chemistry, Michigan State University, East Lansing, MI, 48824

[2]Biomedical Engineering, Michigan State University, East Lansing, MI, 48824

[3]Institute for Quantitative Health Sciences and Engineering, Michigan State University, East Lansing, MI, 48824

[4]Department of Medicine, Duke University, Durham, North Carolina, 27710

[5]Department of Chemistry and Biochemistry, University of Maryland Baltimore County, Baltimore MD, 21250

Abstract

A set of 3D-printed analytical devices were developed to investigate erythrocytes (ERYs) processed in conventional and modified storage solutions used in transfusion medicine. During storage prior to transfusion into a patient recipient, ERYs undergo many chemical and physical changes that are not completely understood. However, these changes are thought to contribute to an increase in post-transfusion complications, and even an increase in mortality rates. Here, a reusable fluidic device (fabricated with additive manufacturing technologies) enabled the evaluation of ERYs prior to, and after, introduction into a stream of flowing fresh ERYs, thus representing components of an *in vivo* ERY transfusion on an *in vitro* platform. Specifically, ERYs stored in conventional and glucose-modified solutions were assayed by chemiluminescence for their ability to release flow-induced ATP. The ERYs deformability was also determined throughout the storage duration using a novel membrane transport approach housed in a 3D-printed scaffold. Results show that hyperglycemic conditions permanently alter ERY deformability, which may explain the reduced ATP release, as this phenomenon is related to cell deformability. Importantly, the reduced deformability and ATP release were reversible in an *in vitro* model of transfusion; specifically, when stored cells were introduced into a flowing stream of healthy cells, the ERY-

spenceda@msu.edu .

Safety: No unexpected, new, and/or significant hazards were associated with this work.

derived release of ATP and cell deformability both returned to states similar to that of non-stored cells. However, after 1–2 weeks of storage, the deleterious effects of the storage were permanent. These results suggest that currently approved hyperglycemic storage solutions are having adverse effects on stored ERYs used in transfusion medicine and that normoglycemic storage may reduce the storage lesion, especially for cells stored for longer than 14 days.

Introduction

Blood components collected for medical use are transfused into patients in need due to trauma, surgery, or as part of therapeutic treatment for disease (such as sickle cell disease, anemia, and cancer).[1–4] According to the most recent National Blood Collection and Utilization Survey Report of 2017, the total number of whole blood and erythrocyte (ERY) transfused annually approached 10.7 million units (not including other blood components) resulting in a stored unit being utilized every 2–3 seconds in the United States.

Despite its role in healthcare, there are some obstacles still facing the field of transfusion medicine. For example, while the risk for viral infections associated with blood transfusion is very low, there is still a risk for bacterial infections and other non-infectious complications such as hemolytic transfusion reactions, transfusion-related acute lung injury, and anaphylaxis.[5] Many reports debate whether the storage duration of the ERY is a determinant of transfusion-associated complications and overall patient outcomes. Koch found that patients who received transfusions of ERYs that were stored for more than two weeks had higher chances for in-hospital mortality, complications occurrence, and even a higher mortality rate one year after transfusion,[6] which was supported by other groups.[7–13] In contrast, several studies have found no statistical difference in overall mortality between fresh ERYs and ERYs stored past two weeks.[14–18] However, a limitation to most, if not all of these studies, is the changes to the ERY immediately upon the addition of the collection and/or storage solutions. If such immediate changes occur, measurement of further changes to the ERY chemical and physical properties during the first few weeks of storage (and continuing throughout storage) would be difficult to determine, thus giving the false appearance that minimal changes occurred to the ERY during storage.

ERYs are stored in solutions that contain very high levels of glucose. One of these solutions, additive solution 1 or AS-1, contains approximately 110 mM glucose; after the addition of the packed ERYs, the glucose concentration is still 40 mM or higher, a level that is nearly 10 times higher than normal glucose concentrations in the circulation.[19] During storage, ERYs undergo various chemical (e.g., increased advanced glycation endproducts or AGEs, increased accumulation of reactive oxygen species) and physical changes (increased cell rigidity, a decrease in cell size) which, collectively, are known as the storage lesion.[20–23] The storage lesion is thought to contribute to post-transfusion complications.

Previously, we reported[24] that reducing the glucose concentrations in storage solutions to a normoglycemic level (and maintaining those levels with periodic feeding of the ERYs during storage) helped maintain many cellular functions of stored ERYs throughout the storage duration and reduce some aspects of the storage lesion, such as sorbitol accumulation.[19] A shortcoming of our previous studies, however, was that we measured many of the

ERY chemical and physical properties in the storage solutions. In contrast, a transfusion would involve taking the stored ERYs and moving them to a human, where the circulation environment is much different than the storage environment. For example, storage solutions do not contain key proteins found in the circulation (such as albumin), the pH is typically lower than the circulation, and, perhaps most importantly, the circulation has a glucose concentration that is much lower than that found in storage solutions.

Therefore, to add rigor to our prior investigations of low glucose storage solutions with periodic feeding, we now report novel discoveries involving key ERY measurements after introducing ERYs (stored in conventional storage solutions such as AS-1 and our modified, normoglycemic solutions (AS-1N)) into a physiological salt solution (PSS) that more closely resembles the *in vivo* circulation. Our results suggest that the negative effects of storage in the hyperglycemic solutions are initially reversible upon dilution in normoglycemic buffers. However, as the ERY storage duration in the hyperglycemic storage solutions approaches 10–14 days, the damage to the ERY is permanent, even upon dilution in normoglycemic PSS.

To facilitate these studies, we also report here the use of multiple 3D-printed devices and demonstrate that ERYs stored in AS-1N prior to transfusion not only perform better in the PSS environment, but also display improved response to key signaling molecules that would be encountered *in vivo*. Specifically, in one construct, we introduce stored ERYs to a rejuvenating solution containing C-peptide and Zn^{2+}, which are both secreted from the pancreatic β-cells *in vivo*.[25] In another construct, we further validate our results by performing a transfusion on-chip and introduce stored ERYs into fresh ERYs collected and purified just hours before merging with the stored cells on a fluidic device. These mixed streams of ERYs were pushed through channels in the absence and presence of INS-1 cells,[26] a rat insulinoma cell line capable of secreting insulin, C-peptide, and Zn^{2+}. Our results suggest that normoglycemic storage solutions reduce properties of the ERY storage lesion. Furthermore, in contrast to most studies in blood banking and transfusion medicine that investigate the effect of the ERY on organ function, the printed tools described here enable us to investigate the effects of the organ and organ function on the stored ERY. Collectively, our studies provide evidence that current storage solutions such as AS-1 inhibit transfused cells from interacting with otherwise properly functioning organs and their secretions *in vivo*; thus, overall performance of the stored ERYs may be enhanced with our normoglycemic (AS-1N) versions of AS-1.

Experimental

Design and Fabrication of the Printed Devices.

All devices were designed using Autodesk Inventor Student Edition (Autodesk, San Rafael, CA) and printed in VeroClear (Stratasys Ltd, Eden Prairie, MN) using an Objet Connex 350 printer (Stratasys) with XY and Z resolution of 100 μm and 16 μm, respectively, housed in the Engineering Department of Michigan State University. The base of the fluidic device is similar to previous designs[27] and contains measurement wells based on standard 96 well plate technology that fits in a standard plate reader. The device contains six channels for sample flow, each of which flows underneath plastic membrane inserts to form a membrane

barrier between the flow and the insert. Supplementary figure S1A shows the printed block device, while S1B displays the cross section of a single channel, enabling a side view of the membrane inserts on a channel, while S1C shows the device in a closed-loop system with a peristaltic pump. Supplementary figure S1D is a representation of the membrane wells alongside static wells not in the flow path. These static wells are used for on-chip calibration of analytes of interest.

A Y-shaped adapter, shown in supplementary figure S2, was used for subsequent studies involving an on-chip transfusion, consisted of three parts: a flow splitter, a controller, and a stopcock. Threads were printed on the parts for easy connection. Prior to use, the three parts were assembled and then the Y-shaped flow splitter was connected to a channel on the fluidic device. The low branch of the flow splitter was connected with the other end of the channel using Tygon tubing, which goes around the rollers of a peristaltic pump. The top branch and the flow controller were connected to a syringe via a male fingertight fitting. Upon injection, the stopcock was adjusted to make the hole (through the stopcock) align with the channel through which liquid can be delivered. The stopcock was rotated 90° to stop delivery of fluids. Teflon tape was used to improve sealing between the stopcock and the controller in some cases. The top branch and the controller need to be prefilled with the liquid to be injected at the beginning of an experiment. Otherwise, trapped air in this component will be injected into the circulation, making the injection amount difficult to quantitatively determine.

Characterization of the i.v. Injection Device.

All reagents were purchased from Sigma-Aldrich (St. Louis, MO) unless specified otherwise. Quantitative injections into the device were characterized by injecting fluorescein solutions into a stream of circulating water. A 50 μL aliquot of fluorescein (300 μM) was injected into a water-filled loop having a volume of 450 μL. The injection was performed by switching the valve for 30 s at a flow rate of 100 μL/min. The liquid was allowed to circulate for 2 min post-injection, after which time, the liquid in the loop (tubing and channel) was collected and the fluorescein concentration was quantitatively determined using fluorescence spectroscopy (ex. 494 nm; em. 521 nm). Based on the injection ratio (1 to 10), the concentration of fluorescein in the loop was expected to be 30 μM. The detected fluorescein concentration was compared with this calculated value, the difference between which can be used as an indicator of injection accuracy. Complications in measurements due to the fluidic device material absorbing fluorescein molecules were overcome by detecting the loss of fluorescence signal intensity of a fluorescein solution after being circulated in a channel for > 1 hour. The distribution of injected fluorescein molecules in the circulating loops was also characterized. Fluorescein was allowed to circulate for 2 minutes following injection, after which, the liquid in the loop was divided into three random sections that were collected in three vials, respectively. If the fluorescein molecules distribute evenly in the loop after an injection, the concentrations in the three parts were expected to be the same. This data is shown in supplementary Tables S1 and S2.

The accuracy of injecting ERYs was also determined. While a 5% ERY sample suspended in PSS was circulating in a loop, a 50 μL aliquot of 50 % ERYs was introduced to the

system by injecting at 100 μL/min for 30 s. The calculated hematocrit of ERYs in the loop after an injection was expected to be 10%. By comparing the detected hematocrit and the calculated value of 10%, injection accuracy of ERYs was determined. In these experiments, counting of ERYs on a hemocytometer was performed to validate measured values in the fluidic device. The distribution of ERYs after an injection was characterized with the same method as that described for fluorescein above, except 5 minutes of circulation time was employed before measuring the hematocrit in the three sections of tubing. This data is shown in supplementary Table S3 and S4.

Fabrication of the 3D-printed Cell Filtration Device.

A filter device was also fabricated using the Objet Connex 350 printer. The main parts of the filter are two flange-shaped slabs that were printed in VeroClear material and contained printed O-rings fabricated in the rubber-like Tango black (Stratasys). A sample inlet was fabricated on the top slab, which was a female fitting with printed threads on the inside. The two slabs can be combined by binder clips, with a piece of semipermeable membrane in between representing the filter, while the printed O-rings on the binding sides of both slabs ensured a secure fit of the membrane without liquid leaking. The engineering sketch of this device is shown in supplementary Figure S3.

ERY Collection, Storage, and Preparation Protocols.

A graphical summary of the blood collection and preparation is shown in supplementary figure S4. Prior to blood collection, solutions for collection and storage were prepared. For whole blood collection, two versions of citrate-phosphate-dextrose (CPD) solutions were prepared; namely the conventional, FDA-approved version of CPD (containing 128.8 mM glucose) or a modified version labeled CPD-N (normoglycemic, containing 5.5 mM glucose). Both CPD solutions also contained 89.4 mM sodium citrate, 15.6 mM citric acid, and 16.1 mM NaH_2PO_4 at pH 5.6. In addition to the collection solutions, two versions of an additive solution were prepared. The FDA approved additive solution 1 (AS-1, 111.1 mM glucose) or a modified, normoglycemic version (AS-1N, 5.5 mM glucose). Both AS-1 and AS-1N also contained 154 mM NaCl, 2.0 mM adenine, and 41 mM mannitol at pH 5.8.

Once the collection and additive solutions were ready for use, 6 non-siliconized and untreated (no anticoagulant) 10 mL glass Vacutainer tubes (BD, Franklin Lakes, NJ) were obtained. A volume of 1 mL of CPD was injected into 3 of the tubes using a syringe, and 1 mL of CPD-N was injected into the remaining 3 tubes. Next, approximately 7 mL of whole blood were collected into each tube from a consented donor. All blood collection procedures from informed and consented donors were approved by the Biomedical and Health Institutional Review Board at Michigan State University. Researchers in the study completed bloodborne pathogen safety training prior to handling blood samples. The blood remained in the collection solutions for 30 minutes at room temperature, approximately 22 °C. All 6 blood-containing tubes were then centrifuged at 2000*g* for 10 minutes, followed by removal of the plasma and buffy coat (white blood cells) layers by aspiration. Purified ERYs from the 3 tubes containing CPD were then combined into a single 15 mL tube, followed by the addition of AS-1 such that the volume ratio of the ERYs to AS-1 was 2:1. The same protocol was followed for ERYs collected in CPD-N and stored in AS-1N. Finally,

2 mL of the ERYs from the tubes (processed in the AS-1 or AS-1N) were added to PVC bags and stored at 4°C. The PVC bags were prepared in-house using rolled PVC (ULINE, Pleasant Prairie WI) and a heat sealer. Prior to use, the PVC bags were sterilized under UV light overnight. All blood collection and storage processes were performed under sterile conditions.

During storage, the ERYs continually consume glucose.[28–30] Therefore, ERYs stored in normoglycemic solution (AS-1N) must be periodically administered glucose to maintain concentrations between 4–6 mM throughout the period of storage.[19, 24] Thus, AS-1N stored cells were "fed" weekly by opening the PVC storage bag and adding 20 μL of 400 mM glucose in saline, and then re-sealing the bag in a sterile environment. The glucose levels in all storage solutions were monitored by a portable glucose meter (Accu-Chek Aviva, Indianapolis, IN). The authors acknowledge this practice would not be feasible in practice but is necessary to investigate our normoglycemic processing solutions.

Fresh ERY samples were prepared for later studies that attempt to mimic an *in vitro* transfusion. These samples were obtained by collecting whole blood from healthy humans into heparinized tubes. The plasma and buffy coat were removed by centrifugation and aspiration. ERYs were then washed 3 times in a normoglycemic physiological salt solution (PSSN, in mM, 4.7 KCl, 2.0 $CaCl_2$, 140.5 NaCl, 12.0 $MgSO_4$, 21.0 tris(hydroxymethyl)aminomethane, 5.5 glucose, and 5% bovine serum albumin (BSA), final pH 7.40).

On each day of experiments, an aliquot of both AS-1 and AS-1N stored ERYs was removed from storage PVC bags and placed in microcentrifuge tubes. ERY hematocrit was then determined by microhematocrit centrifugation with a microhematocrit centrifuge (CritSpin M960–22, StatSpin, Westwood, MA) and a microcapillary reader (StatSpin). Samples were prepared by re-suspending stored ERYs in either PSSN, or hyperglycemic physiological salt solution (PSSH, containing the same components as PSSN with glucose level equal to the extracellular glucose level of 111.1 mM in AS-1 storage bags). Two groups of stored ERY samples were prepared with each group (shown in Table 1) having three samples. The first sample in group one was AS-1N stored ERYs transferred into PSSN to a final hematocrit of 5%, referred to as AS-1N-PSSN sample. The second and third samples were AS-1 stored ERYs transferred to PSSH and PSSN to a same final hematocrit of 5%, referred to as AS-1-PSSH and AS-1-PSSN samples, respectively. The second group of three samples were the same as in the first group (for AS-1-PSSN, AS-1-PSSH, and AS-1N-PSSN) except that all contained 10 nM exogenously added human C-peptide and Zn^{2+}.

Determination of ATP Release and Reversibility.

While an ATP sample is flowing in a channel, ATP diffuses through the membrane into the preloaded buffer in the insert (above the membrane). The ATP collected via diffusion is proportional to the amount of flowing ATP in the channel, and thus by measuring the ATP amount in the preloaded buffer, the ATP in the channel can be determined. The design of static wells between channels enables simultaneous on-chip calibration, which simplifies experimental procedures and improves experimental rigor. The three ERY samples were pumped through the six channels of the device in duplicate, where each

channel formed a closed loop by connecting to soft tubing (the volume of a loop is 450 μL). The circulation in the loops was driven by a peristaltic pump (IDEX Health & Science LLC, Oak Harbor, WA) at a flow rate of 200 μL/min. A 50 μL aliquot of PSS was then loaded in wells above each channel to collect ATP from the flowing ERY samples via diffusion. The entire setup of the pump, the device, and closed loops with circulating samples were then placed in an incubator at 37 °C for 20 minutes to better mimic circulation conditions, after which, the bulk fluidic device was detached from tubing and placed in a spectrophotometer (SpectraMax 4, Molecular Devices, Sunnyvale, CA). The well-established luciferase/luciferin (L/L) chemiluminescence assay was used to detect ATP in the inserts. An aliquot of 10 μL of L/L mixture (prepared by dissolving 2.0 mg of D-luciferin in 5 mL of deionized water and adding 100 mg of firefly extract) was added into the wells simultaneously by a multichannel pipet. After 15 s, the chemiluminescence intensity was detected by the plate reader. To confirm that the increase of released ATP was not due to cell lysis, an absorbance measurement was performed to evaluate if free hemoglobin was detected in the supernatant after flow was concluded. If hemoglobin was detected, that particular sample would be discarded due to indication of lysis. In the studies reported here, there were no samples discarded due to lysis. A calibration curve was obtained for quantification purposes by circulating five ATP standards (concentrations of 0, 100, 200, 300, and 400 nM) prepared in PSS in five randomly chosen channels with identical subsequent detection processes as described above. The device can be reused after simple rinsing with diluted bleach and deionized water. The determination of ATP in the three samples, throughout the 36-day storage, was performed on the same device.

ERY Deformability Measurement Using the 3D-printed Cell Filtration Device.

A piece of polycarbonate membrane with a pore size of 5 μm, which is smaller than the mean diameter (6–8 μm) of ERYs, was used in the filtration device. Only cells with sufficient deformability can go through the membrane and as deformability increases, more cells are expected in the effluent. Tubing for sample introduction was connected to the top slab by screwing the male fingertight adapter at the end of the tubing into the female inlet. The tubing was driven by peristaltic pumping at a pressure of 12 cm H_2O column (~0.17 psi). All three samples of AS-1N-PSSN, AS-1-PSSH, and AS-1-PSSN were measured through the device in a random order. The effluent was collected for 10 minutes, after which, the number of cells in the effluent was counted on the hemacytometer as a measurement of relative ERY deformability.

ELISA-based Determination of C-peptide Uptake by ERYs.

On each day of the experiment, three AS-1N-PSSN, AS-1-PSSN, and AS-1-PSSH samples containing 10 nM exogenously added C-peptide and 7% ERYs were prepared. All three samples were incubated at 37 °C for 2 hours. Next, samples were centrifuged at 500*g* for 5 min, and the supernatant was collected to determine the C-peptide concentration using a C-peptide ELISA (ALPCO, Salem, NH). The ERY C-peptide uptake was calculated by subtracting the moles of C-peptide remaining in the supernatant from the total number of moles added.

Results and Discussion

Determination of ATP Release and Potential for Recovery after Transfer to a Normoglycemic Environment.

ATP also has a well-established role in participating in the regulation and maintenance of blood flow.[31–32] Therefore, maintenance of the concentration of ATP in the circulation is important. We previously reported that ERYs stored in hyperglycemic AS-1 solution released less ATP than those stored in AS-1N.[19, 24] However, the ATP release from those ERYs was measured while the ERYs were still in the AS-1 solution. In an actual transfusion, the AS-1 stored ERYs would be introduced into an environment (the patient circulation) that would have glucose levels closer to 5 mM, which may enable the ERYs to "recover" from their hyperglycemic storage solutions and release normal levels of ATP. This potential for recovery of ATP release from AS-1 stored ERYs was studied using the 3D-printed circulation mimic device. This protocol enables studies that more closely resemble the actual conditions of stored ERYs by circulating samples in a flowing stream at 37 °C after these stored cells had been introduced to a normoglycemic environment (the PSSN). Furthermore, it allows for simultaneous measurements of ERYs stored under various conditions (AS-1 or AS-1N) using a plate reader in a high throughput fashion. All these features make it an ideal platform for flow induced ATP measurements from stored ERYs.

Three experimental trials were conducted as described previously in Table 1. As shown in Figure 1, ATP release from AS-1N-PSSN cells (green bars) was statistically unchanged from day 1 of storage (215 ± 13 nM) thru day 36 of storage (206 ± 11 nM). In comparison, the release of ATP from ERYs stored in the AS-1-PSSH system (grey bars) stayed at a much lower level throughout storage. On the first day of storage, ERYs stored in AS-1-PSSH released 144 ± 8 nM ATP, which was significantly less than AS-1N-PSSN samples and continued to decrease throughout storage to a day 36 value of 90 ± 4 nM. Interestingly, the ATP release from ERYs on day 1 in the AS-1-PSSN environment (222 ± 14 nM, red bars) was statistically equal to the AS-1N-PSSN day 1 value. However, by day 8 the ERY-derived ATP release from the ERYs stored in the AS1-PSSN system began to decrease (167 ± 12 nM) and continued this trend through the end of the study to a value that was equal to those ERYs stored in AS-1 and transferred to PSSH (90 ± 8 nM) ($p < 0.05$).

The results in Figure 1 confirm our previous findings[19, 24] that hyperglycemic storage solutions reduce ERY-derived ATP. Furthermore, these data also now show that the ERYs stored in AS-1 can recover from the hyperglycemic storage conditions, as measured by ATP release from the cells, during early stages of storage. Prior to day 15 of storage, the hyperglycemic (AS-1) stored ERYs were able to recover (completely or at least partially) the ability to release ATP; beyond this point the reversibility or recovery was not observed. Numerous studies and surveys have demonstrated the existence of adverse complications after transfusion and often cite 2 weeks of storage as a turning point in the quality of ERYs.[7–13] It is premature to assume that the inability to recover ATP release from ERYs after 15 days of storage in hyperglycemia is the root cause of these clinical consequences. However, the ATP reversibility trend as a function of storage time and glucose levels in the storage solutions are motivation for further clinical studies investigating these conditions.

Determination of ERY Deformability.

The mechanism describing reduced ATP release from ERYs stored in hyperglycemic solutions remains unknown. However, the mechanism may lie in one of two possible scenarios: hyperglycemic solutions result in less intracellular ATP production, or these solutions affect the ATP release process. Wang[24] reported that intracellular ATP levels in hyperglycemia stored ERYs were higher than those stored in normoglycemic solutions and did not significantly decrease throughout the 36-day storage, which led to the inference that hyperglycemia may adversely alter the ATP release process, rather than reducing intracellular ATP production.

Sprague reported that shear stress induced deformability of ERYs leads to ATP release suggesting that ATP release is related to cell deformability.[33–34] These findings provided a clue to potentially explain the failed ATP reversibility by studying the deformability of stored ERYs. Filtration tests have been widely used to study ERY deformability due to its low instrument requirements and high reproducibility. Because no proper commercial devices were found for this application, 3D-printing, which can model objects with high resolution based on the users' demands, was applied to fabricate a filtration device that minimizes dead volumes, saves the usage of filter membranes and simplifies experimental operation. As shown in Figure 2A, the device is comprised of two slabs, with simultaneously 3D-printed O-rings to seal a piece of semipermeable membrane in between for cell filtration. Due to the small sizes of the O-rings, the dead volume of the filter is minimized to ~ 55 μL. Figure 2B shows the device assembly, which was achieved by clamping the slabs with four binder clips on the wings. Figure 2C demonstrates a real ERY filtration experiment on the device. ERY samples were pumped into the inlet on the top slab and were forced to go through the membrane into the cone shaped chamber in the bottom slab and were collected for cell counting. Cells that had sufficient deformability would deform to pass through the filter, whose pore size (5 μm) was smaller than the cell's diameter (6–8 μm), while less deformable cells would not be able to go through (Figure 2D).

Resuspended AS-1N-PSSN, AS-1-PSSH and AS-1-PSSN cells were evaluated with this method. For a clear data presentation, the cell number in the filter effluent of the AS-1N-PSSN trial on day 1 was set to 100%, and all other collected data were normalized to this 100% value. Supplementary Figure S5 shows the relative increases compared to fresh ERYs as well as controls of C-peptide and Zn^{2+} added alone to the ERYs. As shown in Figure 2E, the deformability of AS-1N-PSSN ERYs maintained constant at around 100% during the whole 36-day storage, while AS-1-PSSN trials kept decreasing from 100% on day 1 to 60% on day 36. The deformability of AS-1-PSSH ERYs also decreased over time, but at a significantly lower level than AS-1N-PSSN. Comparatively, on day 1, AS-1-PSSH cell deformability was 25% lower than AS-1N-PSSN stored cells, while AS-1-PSSN cells completely recovered their deformability after being transfused to normoglycemic PSS. The trend continued until day 8, when deformability of AS-1-PSSN trials decreased to levels similar to AS-1-PSSH trials. After day 8, however, the deformability of AS-1-PSSN cells continued to decrease, without any observed reversibility.

Collectively, the data in Figure 1 and Figure 2 suggest a relationship between deformability and ATP release from stored ERYs used in transfusions. During the first five days of

storage in AS-1, ERY deformability completely recovered after being transferred into a normoglycemic condition, as did the ATP release in Figure 1. On Day 8 and 12, however, the deformability of ERYs did not recover, and the ATP release only partially reversed and was significantly lower than AS-1N-PSSN cells. After 15 days of storage, a permanent alteration of cell deformability and ATP release had occurred. These similarities suggest that hyperglycemia may permanently and adversely alter the deformability of ERYs, which eventually leads to decreased ATP release.

A Potential Rejuvenating Solution Comprised of C-peptide and Zn^{2+}.

Previous work from our group and others indicates that C-peptide, a 31 amino acid peptide secreted from pancreatic β-cells in equimolar amounts with insulin, binds to ERYs and other cell types.[25] When bound to ERYs as part of a complex with albumin and Zn^{2+}, the cell deformability and cell-derived ATP release increased. However, we also reported in the C-peptide/Zn^{2+} studies that these effects are reduced when using ERYs from people with diabetes, who often have a circulation with elevated glucose levels (e.g., between 7–10 mM or higher). Here, we measured the ATP release and deformability of the stored ERYs using the same protocols as those employed to gather the data in Figures 1 and 2. However, just prior to measurement, rather than incubating the ERYs in PSS (either PSSN or PSSH) alone, the ERYs were incubated in these versions of PSS that also contained 10 nM C-peptide and 10 nM Zn^{2+} and then circulated through the channels of the fluidic device or placed in the 3D-printed filtration device in Figure 2.

Data in Figure 1 indicated that 215 ± 13 nM ATP was released from AS-1N-PSSN samples on day 1 of storage, and that value remained stable through the last day of storage (at 206 ± 11). As shown in Figure 3A, ATP release increased to 321 ± 22 nM for samples stored in AS-1N-PSSN that also contained C-peptide and Zn^{2+}. This increase in ATP release from the ERYs was well preserved by the normoglycemic storage condition during the entire period of storage, maintaining a statistically equivalent value of 300 ± 13 nM on day 36 of storage. For the ERYs stored in AS-1-PSSH, the C-peptide/Zn^{2+} rejuvenating strategy was less effective. C-peptide and Zn^{2+} were able to slightly increase the ATP release from ERYs stored in the AS-1-PSSH samples to 163 ± 11 nM on day 1 (in comparison to the 144 ± 8 nM value reported in Figure 1 for the same storage system), but this minor effect became less obvious with time and no longer observed beyond 15 days of storage (90 ± 7 nM). Finally, the data in Figure 3A indicate that the AS-1-PSSN ERYs are initially affected by the C-peptide/Zn^{2+} rejuvenating solution in a positive manner. The day 1 ATP release in AS-1-PSSN samples that also contained C-peptide and Zn^{2+} was 321 ± 6 nM on day 1 and remained above 200 nM for about one week (day 8). However, these ATP values began to decline significantly, decreasing to 84 ± 8 nM on day 36, a value statistically equal to the high glucose system (AS-1-PSSH) on that same day.

The deformability of ERYs stored in the various solution systems and then incubated in C-peptide and Zn^{2+} prior to measurement was similar to the ATP release data. Specifically, the data in Figure 3B suggest that, up to around day 8 of storage, the C-peptide and Zn^{2+} rejuvenating solution was having a positive impact on ERY deformability, even in the high glucose AS-1-PSSH storage system. C-peptide and Zn^{2+} improved the deformability of

AS-1-PSSH samples by 25% on day 1 and 20% on day 5 (in comparison to the same system without C-peptide and Zn^{2+}); however, these increases were no longer measured beyond the first few days. The ERYs stored in the AS-1 and transferred to PSSN revealed a marked increase in deformability on day 1 of 33% ± 2% and 25% ± 3% on day 5 after C-peptide/Zn^{2+} treatment. Not unlike the AS-1-PSSH storage solution, however, the C-peptide/Zn^{2+} rejuvenation strategy had no significant effect on the AS-1-PSSN ERYs beyond day 8. In fact, these two storage solutions were statistically equal at day 12 and the duration of storage. In contrast, the ERYs stored in the AS-1N-PSSN system with periodic feeding of glucose demonstrated a marked response to the C-peptide and Zn^{2+} rejuvenating treatment that remained nearly constant throughout storage (day 1 increase of 36% ± 4% and a day 36 increase of 26% ± 7%).

Not unlike the data in Figures 1 and 2, Figure 3 suggest that ERYs stored in the FDA approved AS-1 solutions do not appear to be affected by the high glucose levels in the AS-1 if transferred or moved to a solution containing normal levels of glucose, as would be the case in a normal transfusion. Importantly, however, if this transfer doesn't occur within the first two weeks (or sooner) of storage, the damage to the ERYs appears to be permanent. The ERY doesn't seem to be able to recover its ability to release ATP and the reduction in its deformability seems to be permanent. The data in Figure 3 also suggest that, in addition to the ERY having some level of permanent damage to its structure and function when stored in AS-1, it also does not respond to physiological cues that would occur in vivo, such as the secretion of key signaling molecules (here, the C-peptide and Zn^{2+}).

In accordance with the data in Figure 3, the data in Figure 4 clearly show that one reason for this failure to respond to the C-peptide and Zn^{2+} is that the ERYs stored in the AS-1 based solutions simply do not bind as well to C-peptide. According to our previous extensive work in this area, about 2 picomoles of C-peptide bind to a 7% solution of ERYs (or about 1,800 molecules of C-peptide per ERY).[25] Here, the data in Figure 4 show that there was an average stable binding of 2.07 ± 0.04 picomoles of C-peptide to ERYs stored in AS-1N-PSSN samples over a 36 day period, a value that is statistically equal to our previous work. Binding of C-peptide to ERYs stored in the AS-1-PSSH resulted in an average of 1.60 ± 0.04 picomoles of C-peptide binding in the first week of storage, which was 25% less compared to AS-1N-PSSN samples. This binding number continued to decrease to less than 1 picomole after day 15. AS-1-PSSN samples bound 2.13 ± 0.14 picomoles of C-peptide on day 1, but beyond day 12, bound values that were statistically equal to the AS-1-PSSH system.

To further improve the experimental rigor leading to the results shown in Figures 3 and 4, we employed a rat insulinoma cell line (INS-1) that secretes insulin, C-peptide, and Zn^{2+}. Thus, as opposed to adding exogenous C-peptide and Zn^{2+} to the stored ERYs (the procedure used to procure data in Figures 3 and 4), the ERYs would be exposed to C-peptide and Zn^{2+} that were secreted from these cells (as well as any other hormones secreted from the INS-1 cells). Rat INS-1 cells were cultured and stimulated in inserts, which were then placed above channels in the 3D-printed device to allow for direct interaction of endogenous C-peptide and Zn^{2+} with ERYs. The data from this experimental design, shown in Figure 5, is consistent with the data in Figures 3 and 4. AS-1N-PSSN samples responded to the INS-1

secretions, with consistently higher ATP release from these ERYs over the entire storage duration (350 ± 26 nM on day 1 and 330 ± 29 nM on day 36) in comparison to the other storage strategies.

Finally, motivated by the results from Figure 5, we employed the microfluidic design described in the methods section to mimic a transfusion of stored ERYs flowing into a stream of fresh ERYs. We employed a 3D-printed, Y-shaped connector with a screw valve to deliver ERYs stored in either AS-1 or AS-1N to a stream of ERYs that were obtained just hours before the experiment was performed. As a control, we also delivered a stream of the fresh ERYs into flowing fresh ERYs. These three streams were delivered into channels containing the INS-1 cells above membranes. Three other identical streams were also pumped through the same device, but into channels that were void of the INS-1 cells (thus, no exposure to C-peptide and Zn^{2+}). As expected, the data in Figure 6 confirm that the ERYs stored in the low glucose AS-1N solution and "transfused" into a stream of fresh ERYs release more ATP than the ERYs stored in FDA-approved AS-1 that were "transfused" into the fresh ERY stream. In fact, the ERYs stored in AS-1N and "transfused" into fresh ERYs released statistically equal amounts of ATP as the fresh ERYs introduced to a separate stream of flowing fresh ERYs for the entire 36-day duration of storage. In contrast, the ATP measured from the stream of ERYs stored in AS-1 and "transfused" into fresh ERYs was statistically less than the other two systems studied on the device. An interesting feature of the data shown in Figure 6 related to the AS-1 stored ERYs is also revealed during these last set of experiments; specifically, in all other data shown in our studies, the AS-1 ERYs were affected long-term (typically after day 12) by the storage, but were able to recover certain attributes (deformability, ATP release, C-peptide binding) when placed in normoglycemic PSS. The results from Figure 6 show that the AS-1 stored ERYs, when introduced to fresh ERYs, underperformed in comparison to AS-1N ERYs from day 1 and remained at that constant, low value throughout storage duration. While more evidence is needed to draw impactful conclusions from this data, it appears that the ERYs stored in AS-1, in addition to undergoing adverse physical and structural changes during storage, may also have a negative impact on fresh ERYs already in the circulation, as confirmed by the decrease in ATP release from the fresh ERYs mixed with ERYs stored in AS-1.

Conclusion

In this study, a set of 3D-printed analytical devices were applied to study ERYs stored in conventional and FDA-approved AS-1 and a modified, normoglycemic version of AS-1, called AS-1N. Specifically, these studies examined the ability of the stored ERYs to recover both functional (ATP release) and structural (relative cell deformability) properties after transfer or *in vitro* transfusion into normoglycemic buffers as a function of duration storage. The ruggedness of the 3D-printed device enabled quantitative determinations of ATP release from stored ERYs throughout the 36-day storage period on the same device, which enhanced the reproducibility and reliability of the results. Our results show that AS-1 stored ERYs cannot recover their ability to release ATP to normal levels after 15 days of storage, while AS-1N stored ERYs retained their ability to release this key signaling molecule, even after 5 weeks of storage. In addition to the 3D-printed circulation fluidic device, we also employed additive manufacturing technology to create a device enabling relative

deformability measurements of the stored ERYs. Similar to ATP release measurements, the AS-1 storage system induced a permanent deformability alteration on stored ERYs after 8 days of storage that was not reversible, even upon transfer to normoglycemic buffer. Finally, our *in vitro* transfusion device confirmed that, not only do the AS-1 stored ERYs not respond to normally functioning cells (in this case, C-peptide and Zn^{2+} secreting rat INS-1 cells), but also the AS-1N stored ERYs perform as well as fresh ERYs when introduced into a stream of flowing, fresh ERYs, even after 5 weeks of storage. These studies will hopefully inform and motivate future *in vivo* studies using the CPD-N/AS-1N storage strategy.

Supplementary Material

Refer to Web version on PubMed Central for supplementary material.

Funding:

This work was funded by the National Heart, Lung, and Blood Institute, HL156440-01A1.

References

1. Estcourt LJ; Kohli R; Hopewell S; Trivella M; Wang WC, Blood transfusion for preventing primary and secondary stroke in people with sickle cell disease. Cochrane Database Syst Rev 2020, 7, CD003146. [PubMed: 32716555]
2. Jones JM; Sapiano MRP; Savinkina AA; Haass KA; Baker ML; Henry RA; Berger JJ; Basavaraju SV, Slowing decline in blood collection and transfusion in the United States - 2017. Transfusion 2020, 60 Suppl 2, S1–S9.
3. Raval JS; Griggs JR; Fleg A, Blood Product Transfusion in Adults: Indications, Adverse Reactions, and Modifications. Am Fam Physician 2020, 102 (1), 30–38. [PubMed: 32603068]
4. Wu HL; Tai YH; Lin SP; Chan MY; Chen HH; Chang KY, The Impact of Blood Transfusion on Recurrence and Mortality Following Colorectal Cancer Resection: A Propensity Score Analysis of 4,030 Patients. Sci Rep 2018, 8 (1), 13345. [PubMed: 30190571]
5. Narayan S; Poles D Serious Hazards of Transfusion (SHOT); 2018.
6. Koch CG; Li L; Sessler DI; Figueroa P; Hoeltge GA; Mihaljevic T; Blackstone EH, Duration of red-cell storage and complications after cardiac surgery. N Engl J Med 2008, 358 (12), 1229–39. [PubMed: 18354101]
7. Biffl WL; Moore EE; Offner PJ; Ciesla DJ; Gonzalez RJ; Silliman CC, Plasma from aged stored red blood cells delays neutrophil apoptosis and primes for cytotoxicity: abrogation by poststorage washing but not prestorage leukoreduction. J Trauma 2001, 50 (3), 426–31; discussion 432. [PubMed: 11265021]
8. Hess JR, Red cell changes during storage. Transfus Apher Sci 2010, 43 (1), 51–9. [PubMed: 20558107]
9. Leal-Noval SR; Jara-Lopez I; Garcia-Garmendia JL; Marin-Niebla A; Herruzo-Aviles A; Camacho-Larana P; Loscertales J, Influence of erythrocyte concentrate storage time on postsurgical morbidity in cardiac surgery patients. Anesthesiology 2003, 98 (4), 815–22. [PubMed: 12657840]
10. Purdy FR; Tweeddale MG; Merrick PM, Association of mortality with age of blood transfused in septic ICU patients. Can J Anaesth 1997, 44 (12), 1256–61. [PubMed: 9429042]
11. Sweeney J; Kouttab N; Kurtis J, Stored red blood cell supernatant facilitates thrombin generation. Transfusion 2009, 49 (8), 1569–79. [PubMed: 19413726]
12. Wang D; Sun J; Solomon SB; Klein HG; Natanson C, Transfusion of older stored blood and risk of death: a meta-analysis. Transfusion 2012, 52 (6), 1184–95. [PubMed: 22188419]
13. Zallen G; Offner PJ; Moore EE; Blackwell J; Ciesla DJ; Gabriel J; Denny C; Silliman CC, Age of transfused blood is an independent risk factor for postinjury multiple organ failure. Am J Surg 1999, 178 (6), 570–2. [PubMed: 10670874]

14. Carson JL; Guyatt G; Heddle NM; Grossman BJ; Cohn CS; Fung MK; Gernsheimer T; Holcomb JB; Kaplan LJ; Katz LM; Peterson N; Ramsey G; Rao SV; Roback JD; Shander A; Tobian AA, Clinical Practice Guidelines From the AABB: Red Blood Cell Transfusion Thresholds and Storage. JAMA 2016, 316 (19), 2025–2035. [PubMed: 27732721]
15. Heddle NM; Cook RJ; Arnold DM; Liu Y; Barty R; Crowther MA; Devereaux PJ; Hirsh J; Warkentin TE; Webert KE; Roxby D; Sobieraj-Teague M; Kurz A; Sessler DI; Figueroa P; Ellis M; Eikelboom JW, Effect of Short-Term vs. Long-Term Blood Storage on Mortality after Transfusion. N Engl J Med 2016, 375 (20), 1937–1945. [PubMed: 27775503]
16. Lacroix J; Hebert PC; Fergusson DA; Tinmouth A; Cook DJ; Marshall JC; Clayton L; McIntyre L; Callum J; Turgeon AF; Blajchman MA; Walsh TS; Stanworth SJ; Campbell H; Capellier G; Tiberghien P; Bardiaux L; van de Watering L; van der Meer NJ; Sabri E; Vo D; Investigators A; Canadian Critical Care Trials, G., Age of transfused blood in critically ill adults. N Engl J Med 2015, 372 (15), 1410–8. [PubMed: 25853745]
17. Steiner ME; Ness PM; Assmann SF; Triulzi DJ; Sloan SR; Delaney M; Granger S; Bennett-Guerrero E; Blajchman MA; Scavo V; Carson JL; Levy JH; Whitman G; D'Andrea P; Pulkrabek S; Ortel TL; Bornikova L; Raife T; Puca KE; Kaufman RM; Nuttall GA; Young PP; Youssef S; Engelman R; Greilich PE; Miles R; Josephson CD; Bracey A; Cooke R; McCullough J; Hunsaker R; Uhl L; McFarland JG; Park Y; Cushing MM; Klodell CT; Karanam R; Roberts PR; Dyke C; Hod EA; Stowell CP, Effects of red-cell storage duration on patients undergoing cardiac surgery. N Engl J Med 2015, 372 (15), 1419–29. [PubMed: 25853746]
18. van de Watering L; Lorinser J; Versteegh M; Westendord R; Brand A, Effects of storage time of red blood cell transfusions on the prognosis of coronary artery bypass graft patients. Transfusion 2006, 46 (10), 1712–8. [PubMed: 17002627]
19. Mu R; Chen C; Wang Y; Spence DM, A quantitative, in vitro appraisal of experimental low-glucose storage solutions used for blood banking. Analytical Methods 2016, 8 (38), 6856–6864.
20. Glynn SA, The red blood cell storage lesion: a method to the madness. Transfusion 2010, 50 (6), 1164–9. [PubMed: 20598098]
21. Glynn SA; Klein HG; Ness PM, The red blood cell storage lesion: the end of the beginning. Transfusion 2016, 56 (6), 1462–8. [PubMed: 27080455]
22. Roback JD, Vascular effects of the red blood cell storage lesion. Hematology Am Soc Hematol Educ Program 2011, 2011, 475–9. [PubMed: 22160077]
23. Roussel C; Dussiot M; Marin M; Morel A; Ndour PA; Duez J; Le Van Kim C; Hermine O; Colin Y; Buffet PA; Amireault P, Spherocytic shift of red blood cells during storage provides a quantitative whole cell-based marker of the storage lesion. Transfusion 2017, 57 (4), 1007–1018. [PubMed: 28150311]
24. Wang YM; Giebink A; Spence DM, Microfluidic evaluation of red cells collected and stored in modified processing solutions used in blood banking. Integr Biol-Uk 2014, 6 (1), 65–75.
25. Geiger M; Janes T; Keshavarz H; Summers S; Pinger C; Fletcher D; Zinn K; Tennakoon M; Karunarathne A; Spence D, A C-peptide complex with albumin and Zn(2+) increases measurable GLUT1 levels in membranes of human red blood cells. Sci Rep 2020, 10 (1), 17493. [PubMed: 33060722]
26. Acosta-Montalvo A; Saponaro C; Kerr-Conte J; Prehn JHM; Pattou F; Bonner C, Proglucagon-Derived Peptides Expression and Secretion in Rat Insulinoma INS-1 Cells. Front Cell Dev Biol 2020, 8, 590763. [PubMed: 33240888]
27. Liu Y; Chen C; Summers S; Medawala W; Spence DM, C-peptide and zinc delivery to erythrocytes requires the presence of albumin: implications in diabetes explored with a 3D-printed fluidic device. Integr Biol (Camb) 2015, 7 (5), 534–43. [PubMed: 25825241]
28. Beutler E; West C, The storage of hard-packed red blood cells in citrate-phosphate-dextrose (CPD) and CPD-adenine (CPDA-1). Blood 1979, 54 (1), 280–4. [PubMed: 444671]
29. Hussein E; Enein A, Clinical and quality evaluation of red blood cell units collected via apheresis versus those obtained manually. Lab Med 2014, 45 (3), 238–43. [PubMed: 25051076]
30. Picker SM; Radojska SM; Gathof BS, In vitro quality of red blood cells (RBCs) collected by multicomponent apheresis compared to manually collected RBCs during 49 days of storage. Transfusion 2007, 47 (4), 687–96. [PubMed: 17381628]

31. Sprague RS; Ellsworth ML; Stephenson AH; Lonigro AJ, ATP: the red blood cell link to NO and local control of the pulmonary circulation. Am J Physiol 1996, 271 (6 Pt 2), H2717–22. [PubMed: 8997335]

32. Sprague RS; Stephenson AH; Ellsworth ML; Keller C; Lonigro AJ, Impaired release of ATP from red blood cells of humans with primary pulmonary hypertension. Exp Biol Med (Maywood) 2001, 226 (5), 434–9. [PubMed: 11393171]

33. Sprague RS; Olearczyk JJ; Spence DM; Stephenson AH; Sprung RW; Lonigro AJ, Extracellular ATP signaling in the rabbit lung: erythrocytes as determinants of vascular resistance. Am J Physiol Heart Circ Physiol 2003, 285 (2), H693–700. [PubMed: 12689860]

34. Sprung R; Sprague R; Spence D, Determination of ATP release from erythrocytes using microbore tubing as a model of resistance vessels in vivo. Anal Chem 2002, 74 (10), 2274–8. [PubMed: 12038751]

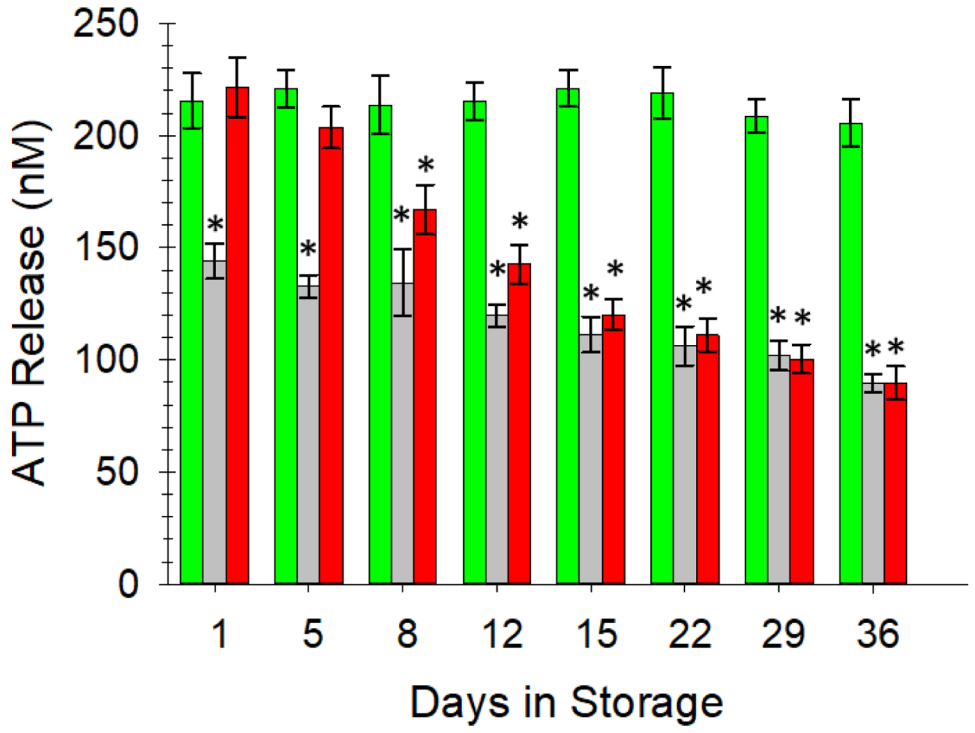

Figure 1.

Flow-induced release of ATP from ERYs stored in various additive solutions and transferred to various buffer systems prior to introduction to the fluidic device. The green bars, representing our normoglycemic AS-1N transferred into a normoglycemic physiological salt solution (PSSN) maintained ATP release levels above 200 nM throughout storage. ERYs stored in AS-1 and moved to a hyperglycemic PSS (PSSH), represented by the gray bars, released significantly less ATP than AS-1N stored ERYs and continued to decrease throughout storage duration. AS-1 stored ERYs after transfer to PSSN (red bars), initially released statistically equivalent amounts of ATP until day 8, after which the ERYs released less ATP, eventually settling to a value that was statistically equal to the AS-1-PSSH system. This data suggest that the FDA-approved AS-1 storage solution may be damaging to the stored ERYs and that the damage is non-reversible after two weeks of storage. Error bars are ±SEM, n=6 for all, *$p<0.05$ to AS-1N-PSSN day 1.

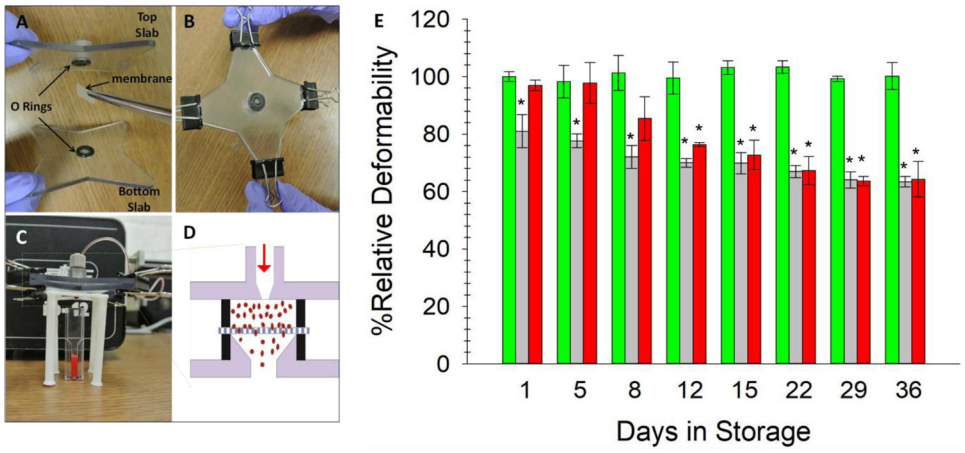

Figure 2:

3D-printed Cell Filter Device for ERY Deformability Measurements. **A)** The two 3D-printed slabs with holes in the center for O-ring fittings, plus the addition of the 5 μm polycarbonate membrane. **B)** The two slabs and membrane are secured using binder clips on the four wings. **C)** A view of the assembled device and experimental set-up. The sample is introduced through the fitting in the top slab and forced through the membrane using a peristaltic pump. Only cells with sufficient deformability will pass through the filter. The cells are then counted with a hemocytometer. **D)** A schematic cross view of the filtration process within the device. **E)** AS-1N-PSSN samples (green bars) possessed the highest deformability and maintained a stable level throughout 36 days of storage. AS-1-PSSH samples (light grey bars) showed the least deformability, which also decreased with time. Deformability of ERYs in AS-1-PSSN samples (red bars) were able to completely recover (day 8) to a normal level of deformability or were no longer able to recover (beyond day 12) upon transfer to PSSN. Error bars are ±SEM, n≥3, *p<0.05 to AS-1N-PSSN day 1.

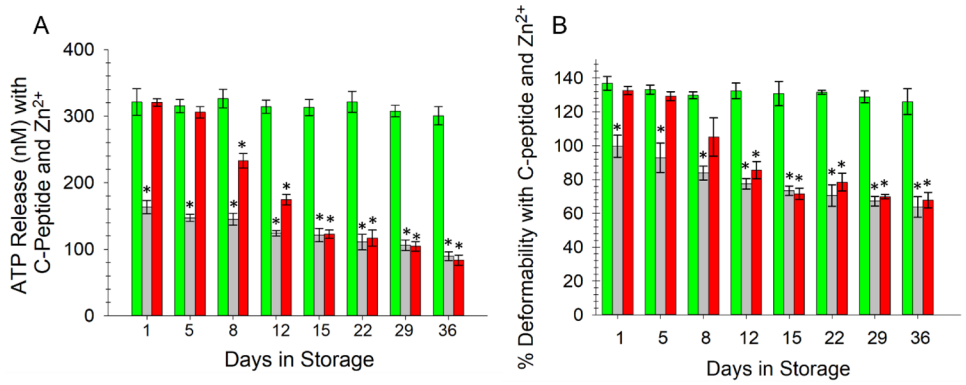

Figure 3.

ERY release of ATP and relative deformability after addition of a C-peptide and Zn^{2+} rejuvenating solution. **A)** ERY-derived ATP was measured in a similar manner to that described to obtain data in Figure 1; however, prior to flowing ERYs through the fluidic device, all ERYs were incubated with various forms of PSS that contained C-peptide and Zn^{2+}. ATP release from ERYs stored in the AS-1N-PSSN environment (green bars) increased to values above 300 nM and remained statistically equal to day 1 values throughout the 36-day storage period. AS-1-PSSH samples (gray bars) did not respond to C-peptide and Zn^{2+}, showing a slight increase in day 1 values from similar samples in Figure 1 but remaining well below the values from the AS-1N stored ERYs. ATP release from AS-1-PSSN samples (red bars) was increased to 300 nM until day 5, after which the values were significantly reduced. **B)** An almost identical trend was measured for deformability of the ERYs stored in the same systems. Error bars are ±SEM, n=6 for all, *$p<0.05$ to AS-1N-PSSN day 1 of the respective graph.

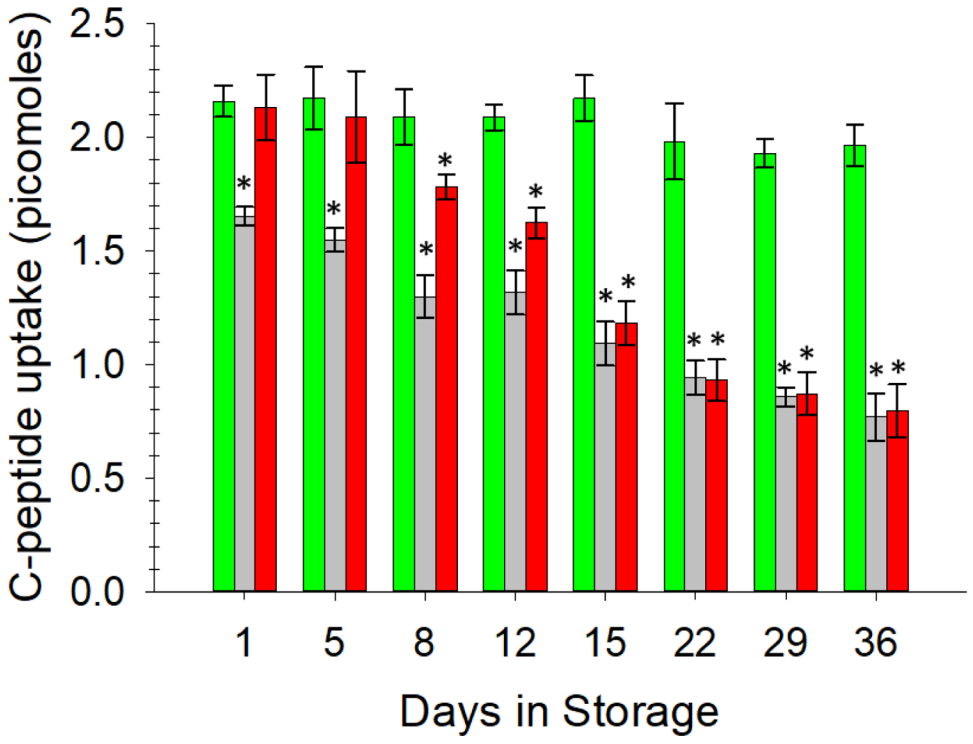

Figure 4.

ELISA determination of C-peptide uptake by stored ERYs transferred to various buffer systems. A constant, ~2 pmol amount of C-peptide binding to ERYs was measured in the AS-1N-PSSN system (green bars). C-peptide binding to ERYs in the AS-1-PSSH samples (light grey bars) continued to decrease over time. C-peptide binding to ERYs in the AS-1-PSSN samples (red bars) were statistically equal to the AS-1N system in the first 5 days and partially reversed until day 12 but did not recover to bind equal amounts of C-peptide after day 15. Error bars are ±SEM, n≥5, *p<0.05 to AS-1N-PSSN on day 1.

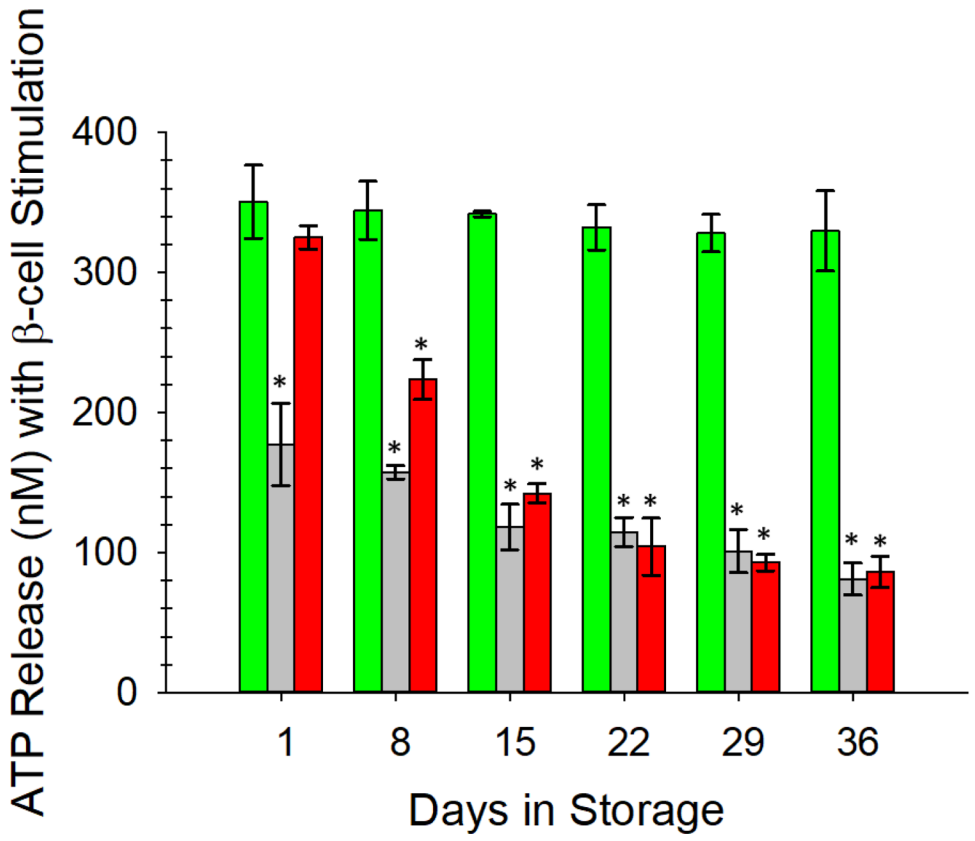

Figure 5.

Response of stored ERYs to β-cell-like secretions from rat INS-1 cells as determined by ERY-derived ATP. AS-1N-PSSN samples (green bars) responded to β-cells in a manner similar to the direct addition of exogenous C-peptide and Zn^{2+}. ERYs stored in the AS-1-PSSH solutions (gray bars) responded with significantly less release of ATP, suggesting less binding of the C-peptide and Zn^{2+} to these ERYs in hyperglycemic solutions. Response of AS-1-PSSN samples (red bars) to secretions followed a similar pattern as data shown in other figures; specifically, the high glucose levels in the AS-1 were overcome upon addition to PSSN. However, beyond day 8 of storage in the AS-1, the ERYs were unable to fully recover in the normoglycemic PSSN. Error bars are ±SEM, n=3 for all, *$p<0.05$ to AS-1N-PSSN day 1.

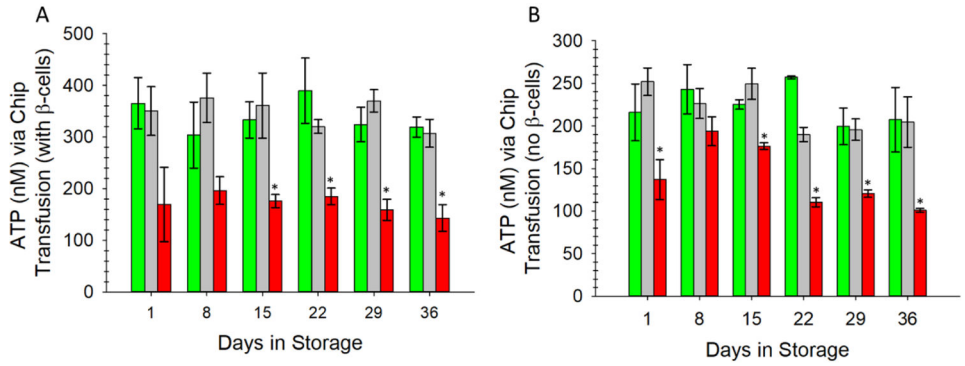

Figure 6.

Fresh ERYs were circulated through the fluidic device with a peristaltic pump containing a unique mechanical screw valve on the top part of a Y-shaped connector at the device channel entrance (see supplementary figure S5). This valve enabled an on-chip transfusion of stored ERYs in AS-1N (green bars), fresh ERYs (gray bars), or ERYs stored in AS-1 (red bars) into a stream of fresh ERYs that were collected just prior to experiment. Furthermore, in (**A**) the ERYs were delivered through channels underneath membrane inserts containing the INS-1 cells (thus, these ERYs were subjected to C-peptide and Zn^{2+} secretions. The same device had 3 other channels accepting similar ERY systems but without INS-1 cells (**B**). ATP was measured downstream in separate transwell inserts. In (**A**), note the level of ATP release (> 300 nM for the entire duration) for the ERYs stored in AS-1N and merged with the fresh ERYs that were subjected to the INS-1 secretions. These values are statistically equal to fresh ERYs merged with a separate stream of the same fresh ERYs each day of the study. The AS-1 ERYs showed much less ATP release when merged with the fresh ERYs throughout storage duration. A similar trend is shown in (**B**) for each storage set, although the ATP release is lower, presumably from having no C-peptide/Zn^{2+} secretions due to the absence of the INS-1 cells. Error bars are ±SEM, n=3 for all, *$p<0.05$ to AS-1N-PSSN day 1.

Table 1:

ERY Storage Sample Conditions. The conditions of the solution that ERYs were stored in and the solution that ERYs were added to post storage.

Name	Storage Solution [Glucose]	Preparation
AS-l-PSSN	111.1 mM	ERYs stored in AS-l transfused into PSSN
AS-1-PSSH	111.1 mM	ERYs stored in AS-l transfused into PSSH
AS-1N-PSSN	5.5 mM	ERYs stored in AS-1N and transfused into PSSN